580–587 Nucleic Acids Research, 1995, Vol. 23, No. 4 © 1995 Oxford University Press

Bulged-out nucleotides in an antisense RNA are required for rapid target RNA binding *in vitro* and inhibition *in vivo*

Tord Å. H. Hjalt and E. Gerhart H. Wagner*

Department of Microbiology, Biomedical Center, Uppsala University, Box 581, S-751 23 Uppsala, Sweden

Received December 5, 1994; Revised and Accepted January 9, 1995

ABSTRACT

Naturally occurring antisense RNAs in prokaryotes are generally short, highly structured and untranslated. Stem–loops are always present, and loop regions serve as primary recognition structures in most cases. Single-stranded tails or internal unstructured regions are required for initiation of stable pairing between antisense and target RNA. Most antisense RNAs contain bulged-out nucleotides or small internal loops in upper stem regions. Here we investigated the role of the bulged-out nucleotides of CopA (the copy number regulator of plasmid R1) in determining the binding properties of this antisense RNA to its target *in vitro* and the efficiency of a translational inhibition *in vivo*. The introduction of perfect helicity in the region of the two bulges in CopA decreased pairing rate constants by up to 180-fold, increased equilibrium dissociation constants of the 'kissing intermediate' up to 14-fold, and severely impaired inhibition of *repA* expression. A previously described loop size mutant of CopA showed decreased pairing rates, but, in contrast to the bulge-less mutant CopAs, shows a decreased dissociation constant of the 'kissing complex'. We conclude that removal of the specific bulges/internal loops within the stem–loop II of CopA impairs the inhibitor, and that creation of an internal loop at a different position does not restore activity, emphasizing the optimal folding of wild-type CopA. The accompanying paper shows that an additional function of bulges can be protection from RNase III cleavage.

INTRODUCTION

Antisense RNA-mediated regulation occurs in many prokaryotic systems, notably in accessory genetic elements: phages, transposons and plasmids (1). The majority of antisense RNAs have been identified as plasmid copy number regulators. These antisense RNAs are inhibitors that act at the post-transcriptional level. In the ColE1-plasmid family, RNAI inhibits primer maturation (2), whereas in plasmids of the IncFII-like and IncIα/IncB families, antisense RNAs inhibit translation of a Rep protein (3–7). In plasmids of Gram-positive hosts, like pT181 and pIP501, antisense RNAs induce transcriptional attenuation (8,9). In all these systems, antisense RNAs are extremely efficient inhibitors. For proper antisense RNA function, its intracellular concentration must represent a measure of the current plasmid concentration. This is ensured by constitutive synthesis and a short half-life, i.e., deviations from average copy number entail rapid changes in antisense RNA concentration, and inhibition of the replication rate-limiting step (synthesis of primer/Rep protein) is regulated by a negative feedback loop [for a recent review, see (10)].

The antisense RNAs encoded by many plasmids show high *in vitro* binding rates to their respective target RNAs. The pairing rate constants obtained for the antisense/target RNA pairs of ColE1 (11), R1 (12), pMU720 [IncB; (13)] and ColE2 (14) are of the order $10^6\ M^{-1}\ s^{-1}$, which are the highest values obtained for any antisense/target RNA system studied. Studies of the kinetics of pairing, and elucidation of earlier steps in the pairing pathway, indicated that the values obtained may be upper limits, since the formation of (one of) the first intermediate(s)—the so-called kissing complex—appears to be rate-limiting. This implies that the binding follows a Briggs–Haldane kinetic scheme. In general, the binding process starts by a loop–loop interaction (kissing complex), and complete pairing requires a second interaction that involves single-stranded regions involving, e.g., the 5′-tail of RNAI of ColE1 and a stretch of nucleotides between stem–loops I and II of CopA of R1, respectively.

In addition to the recognition stem–loops and the single-stranded regions required for complete pairing, antisense RNAs often carry internal loops and bulged-out nucleotides within the upper stems and close to the loop. This is most pronounced in antisense RNAs that have been shown to carry only one stem–loop involved in the target recognition step, i.e. CopA of R1 [and antisense RNAs in other IncFII-related plasmids; (15)], Inc RNA of IncIα/IncB plasmids (16), and also RNA-OUT of *IS*10 (17). What is the significance of bulged-out nucleotides and internal loops? One can conceive of three main possibilities: (i) interrupted intra-strand helicity could protect RNAs from cleavage by RNase III, (ii) bulges may be recognition sites for proteins that affect antisense RNA-mediated control [e.g. Rom; (18,19)], and (iii) bulges could facilitate the binding process between antisense and target RNA. Here we analyzed whether the removal of either one, or both, of the bulges in CopA affects binding to

* To whom correspondence should be addressed

CopT. It is shown that pairing rate constants of CopA/CopT mutant pairs are strongly decreased *in vitro*. Similarly, the stability of the 'kissing complex' between CopI (only consisting of stem–loop II of CopA) and CopT is decreased in the mutants. This is paralleled by the results from *repA-lacZ* expression *in vivo*, where the mutant CopAs were very poor inhibitors. The data presented may indicate that bulges facilitate the pairing process through the transient formation of the kissing intermediate that involves the breakage of base-pairs in the upper CopA stem II, or that bulges are required for a structural rearrangement that aligns the single-stranded regions in CopA and CopT for initiating stable pairing. Alternative pathways for mutant CopA/CopT pairing are discussed.

The accompanying paper (20) addresses the question of metabolic stability of CopA in the presence and absence of bulges, and reports that bulges protect CopA from cleavage by RNase III.

MATERIALS AND METHODS

Strains and plasmids

The *Escherichia coli* strain MC1061 [*araD139, (Δara-leu)7697, lacZ74, galU, hsdR, rpsL*; (21)] was used for plasmid constructions. For β-galactosidase assays, the RNase III-deficient strain IBPC-*rnc14*::*Tn*10 (20) and its wild-type parent IBPC5321 [F⁻, *thi-1, argG6, argE3, his-4, mtl-1, xyl-5, tsx-29, rpsL, ΔlacX74*; (22)] were used, respectively. The plasmids carrying *repA-lacZ* translational fusions (used for *in vivo* β-galactosidase assays) were derived from pGW177-L (3). For construction of mutant derivatives of this plasmid, the unique *BglII–SalI* fragment of the wild-type pGW177-L was replaced by the corresponding fragments from pGW58-derivatives carrying the mutated *copA* genes [see Table 1 in the accompanying paper (20)]. The resulting plasmids were denoted pGW177-Lo-L, -Up-L, -L/U-L and -Xb-L. All these plasmids carry intact *copA* and *repA* promoters, respectively. For an analysis of derepressed *repA-lacZ* expression, mutation III (23) was introduced into pGW177-L and pGW177-L/U-L, respectively, as described in Blomberg *et al.* (24). Mutation III inactivates the *copA* promoter without abolishing translational coupling between *tap* and *repA*. These plasmids are denoted pGW177-III-L and pGW177-III-L/U-L, respectively.

Preparation of CopT, CopI and CopA RNA

In vitro transcription of CopT and CopA RNAs by T7 RNA polymerase was done on PCR-generated templates, whereas CopI RNAs were transcribed from plasmids of the pGW16-series, linearized with the restriction enzyme *Dra*I. The protocol for transcription and isolation of the RNAs is given in the accompanying paper (20).

Determination of CopA/CopT pairing rate constants

Pairing rate constants of CopA/CopT pairs were calculated from gel shift assays as described previously (12,25).

Determination of equilibrium dissociation constants of CopI/CopT pairs by native gel electrophoresis

Kissing complex formation between CopT and truncated CopA variants, unable to proceed to stable duplex formation, has been demonstrated on native gels (26,27). Using this assay, we determined CopI/CopT equilibrium dissociation constants analogous to experiments performed by Pyle *et al.* (28). CopI [see fig. 1 in the accompanying paper (20)] essentially represents a stem–loop II without single-strand extensions. Uniformly [α-^{32}P]UTP-labelled CopI RNAs of wild-type or mutant origin at a final concentration of 0.13 nM were incubated with an excess of ^{3}H-labelled (homologous) CopT at increasing concentrations, as indicated in Figures 3 and 4. Incubation was at 37°C for 10 min in 10 µl of TMN buffer (20 mM Tris–acetate pH 7.5, 10 mM Mg-acetate, 100 mM NaCl). Five µl of loading buffer (TMN, but containing 30% glycerol, 0.05% bromophenol blue, 0.05% xylene cyanol, 0.4 mg/ml of yeast tRNA) was added prior to loading onto 7% native gels. Gels were run in TMN buffer at 100 V for 3.5 h at 4°C with buffer recirculation. Dried gels were subsequently analysed by autoradiography to obtain the photographs in Figure 3. The signals corresponding to CopI and the kissing complex, respectively, were quantified using a Molecular Dynamics PhosphorImager 400S.

Kinetic determination of the dissociation constant of the CopI/CopT binding intermediate

Association and dissociation rate constants of the loop–loop intermediate (kissing complex) can be determined by preincubating an excess of truncated CopAs with labelled CopT (as competitive inhibitor), followed by binding of an even greater excess of CopA over CopT. Truncated CopAs formed kissing complexes with CopT, and were only slowly converted to duplexes, so that free CopT (i.e. the fraction of $CopT_o$ that was not engaged in the kissing complex) could be measured by determining the much faster rate of CopA/CopT duplex formation (27). If the inhibitory RNA is completely impaired in pairing, a maximum inhibition level will be reached that is related to the K_d of the kissing intermediate. We therefore used CopI as an inhibitor instead of the truncated CopA species used by Persson *et al.* (27). Uniformly labelled CopT was preincubated with a defined concentration of unlabelled CopI (at least 10-fold excess over CopT) for various periods of time. After preincubation, an aliquot was withdrawn and incubated with unlabelled CopA RNA (at least 10-fold excess over CopI). After additional short time intervals, the kinetics of CopA/CopT duplex formation was analyzed by gel shift analysis on denaturing gels (27). The CopI-dependent decrease in CopA/CopT binding rate permits calculation of K_d. Based on pilot experiments, we chose to determine CopI/CopT dissociation constants in assays of 30 min preincubation time, using CopI concentrations at or close to the K_d values obtained for each CopI/CopT mutant or wild-type combination in the gel-shift assay on native gels (Fig. 3). In the cases where this experimental protocol was feasible (see Results), the K_d values were calculated from the decrease in the pseudo-first order binding rate constant k' that was due to CopI/CopT kissing complex formation (27). Since the ratio:

$$k'_{(\text{presence of CopI})}/k'_{(\text{absence of CopI})}$$

is equivalent to the ratio:

$$CopT_{free}/CopT_o,$$

this permits calculation of K_d from:

$$K_d = \frac{([T_o]-[C]) \times ([I_o]-[C])}{[C]}$$

where T_o is the initial concentration of labelled CopT, I_o the initial concentration of CopI, and C the concentration of the kissing complex as calculated above.

In vivo repA-lacZ expression assays

RepA-LacZ fusion protein synthesis was measured in cell extracts of overnight cultures. The protocol used for the experiments in Table 2 was essentially as in Berzal-Herranz *et al.* (29), with the modification that cell extracts were made from cultures grown in minimal medium with 0.2% casamino acids and 0.2% glucose.

RESULTS

The bulged-out nucleotides in CopA are required for rapid pairing

We used site-directed mutagenesis to change nucleotides in the *copA* gene resulting in restored base-pairing in the CopA bulge regions. From these mutant plasmids we could generate templates for transcription of purified CopA and CopT RNAs for binding assays. The mutational changes in the CopA-species used are depicted in figure 1 of the accompanying paper (20). Homologous CopA/CopT RNA pairs of either wild-type or mutant origin were analyzed for pairing rates using a gelshift assay. Autoradiograms of such assays are shown in Figure 1. Pairing rate constants (k_{app}) were calculated as described (12), and are summarized in Table 1. Most surprisingly, pairing rate constants of mutant CopA/CopT pairs were decreased by 44- to 185-fold compared to the wild-type pair. This pairing defect by far exceeds any effect found in studies of CopA/CopT pairs in which base changes were located in the primary recognition loop (12; Wagner, unpublished).

Since the mutants RNA pairs performed so poorly in the pairing assay, we tested whether binding still followed second-order kinetics, i.e. whether the overall binding rates were dependent on the concentration of the RNA component present in excess (12). Figure 2 shows such a C_ot-experiment for two CopA/CopT mutant pairs (L/U and Xb, respectively). As can be seen, over a large concentration range the rate of RNA duplex formation increased in proportion to the concentration of CopT (which was in great excess over labelled CopA), such that the product of [CopT] × time remained essentially constant. The same result was obtained previously for the wild-type CopA/CopT pair (12). In conclusion, this analysis shows no clear indication that a change in rate-limiting step has taken place.

Pairing rate determinations of heterologous CopA/CopT combinations showed that CopA-Wt paired almost equally well with its homologous target as with CopT-L/U, whereas CopA-L/U showed almost equally low pairing rates with its homologous target and the heterologous CopT-Wt, indicating that the pairing defect caused by the L/U mutation inactivates CopA (data not shown).

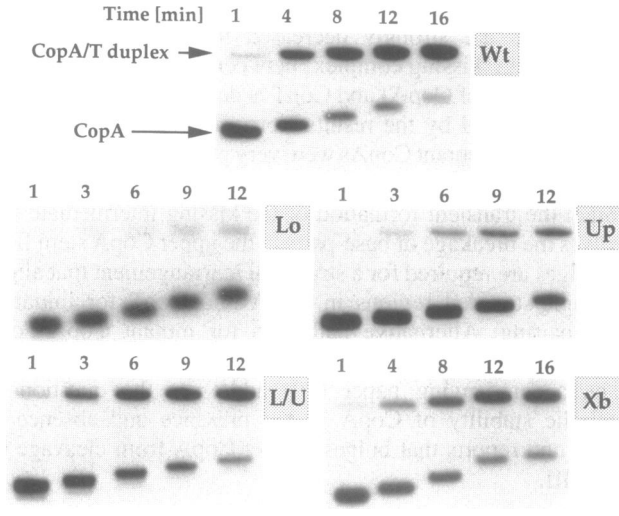

Figure 1. *In vitro* pairing assays. Time courses of binding between homologous CopA/CopT pairs were performed according to (12) and Materials and Methods. CopA (concentrations used $<10^{-10}$ M in all cases) was uniformly labelled, and CopT was tritiated and in high excess. Electrophoretic separation of free CopA and CopA/CopT duplex was done on 8% denaturing gels. Samples were loaded onto a running gel immediately after aliquots were quenched in loading buffer. The concentrations of CopT were for the different incubations: 2.0×10^{-9} M (Wt); 9.4×10^{-9} M (Lo); 9.2×10^{-9} M (Up); 1.1×10^{-7} M (L/U); 1.8×10^{-7} M (Xb).

Table 1. Determination of pairing rate constants and relative K_d values of wild-type and mutant CopA/CopT and CopI/CopT pairs

CopA/CopT RNAs used	k_{app} (M^{-1} s^{-1})[a]		Impairment relative to wt RNA pair[b]	CopI/ CopT RNAs used	K_d (M)[c]		Increase relative to wt RNA pair[d]
Wt	1.3×10^6	[± 37%]	1 ×	Wt	7.4×10^{-9}	[± 32%]	1 ×
Lo	1.8×10^4	[± 22%]	72 ×	Lo	1.0×10^{-7}	[± 0%]	14 ×
Up	2.9×10^4	[± 42%]	44 ×	Up	5.7×10^{-8}	[± 25%]	8 ×
L/U	1.4×10^4	[± 24%]	91 ×	L/U	4.6×10^{-8}	[± 35%]	6 ×
Xb	6.9×10^3	[± 22%]	185 ×	Xb	5.5×10^{-8}	[± 45%]	7 ×
6C	2.2×10^5	[± 39%]	6 ×	6C	4.0×10^{-10}	[± 25%]	0.05 ×

[a]Binding rate constants were calculated from time courses of binding like those shown in Figure 1 (12; Materials and Methods). Five independent determinations were performed, average values are given, and standard deviations are represented in brackets.

[b]The relative impairment is the k_{app}(Wt)/k_{app}(Mut) ratio.

[c]Equilibrium dissociation constants (K_d) were determined by native gel electrophoresis from experiments as those shown in Figure 3 and represent the average of two independent experiments. Standard deviations are given as percentages.

[d]K_d values of the mutant pairs were divided by that of the wild-type pair.

Table 2. Expression of *repA-lacZ* in cells carrying wild-type or mutant translational fusion plasmids

	rnc$^+$ host strain[a]		*rnc*$^-$ host strain[a]	
Plasmids with intact *copA* promoter				
none	<0.1	[± 0%]	<0.1	[± 0%]
pGW177-L	1.0	[± 15 %]	1.0	[± 37 %]
pGW177-Lo-L	23.3	[± 11%]	12.8	[± 19%]
pGW177-Up-L	19.2	[± 9%]	6.5	[± 16%]
pGW177-L/U-L	10.6	[± 17%]	8.0	[± 8%]
pGW177-Xb-L	23.3	[± 12%]	10.2	[± 12%]
Plasmids with inactive *copA* promoter				
pGW177-III-L	26.0	[± 17%]	10.7	[± 20%]
pGW177-III-L/U-L	13.7	[± 12%]	6.0	[± 27%]

[a]The genotype of the host strains for the fusion plasmids is shown in the Materials and Methods. Assays were performed as described in the Materials and Methods. Activities (averages of three independent experiments) are relative values, and standard deviations are given as percentages. The β-galactosidase activities of each strain carrying the wild-type plasmid is set to unity. Note that the activities in the *rnc*$^-$ mutant strain were approximately five times higher than in the wild-type strain.

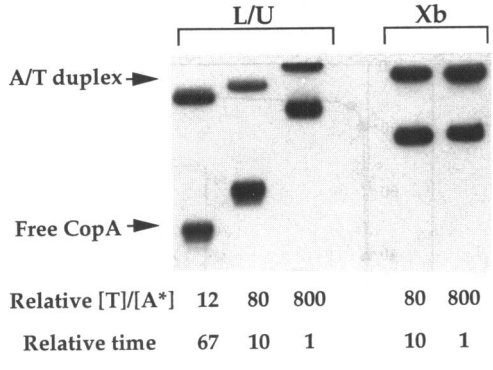

Figure 2. CopA/CopT pairing rate as a function of CopT concentration. Two mutant CopA/CopT pairs were tested. CopA was uniformly labelled and present at 2.4 × 10^{-10} M. CopT was in excess as indicated. Samples were stopped at times such that the product of [CopT] × time was constant (C_0t = constant). Stopped samples were immediately applied to a running gel.

Bulge mutations result in decreased stability of the kissing intermediate

We synthesized uniformly labelled CopI RNAs (consisting only of stem–loop II of CopA) of mutant or wild-type origin [see fig. 1 in the accompanying paper (20)]. Aliquots of CopI were incubated with CopT at increasing concentrations, and kissing complex formation was analyzed on native gels. CopI is severely impaired in complete pairing, but forms a kissing complex when incubated with its homologous target RNA (26). Figure 3 shows autoradiograms of gels used for the quantitation of kissing complexes as a function of [CopT], and plots in which the fraction of labelled CopI in the kissing complex is graphically represented. The concentration of CopT at which half of the labelled CopI would be found migrating as the loop–loop intermediate was determined from each graph. These values represent relative dissociation constants (K_d) and are depicted in Table 1. It is clear that K_d values of all bulge mutant CopI/CopT pairs are strongly increased (6- to 14-fold; Table 1). In contrast, analysis of the loop size mutant 6C (25) yielded a K_d that was almost 20-fold lower than that of the wild-type CopI/CopT pair. In conclusion, as can be seen in the schematic summary in Figure 4, the removal of bulges affects both the pairing rates between CopA and CopT and the equilibrium dissociation constants between CopI and CopT. However, pairing rate is, in all cases, much more affected than the stability of the binding intermediate.

A kinetic determination of the dissociation constant of the kissing complex is not feasible for bulge mutant RNA pairs

The K_d values obtained in the native gel migration assay (Fig. 3; Table 1) could represent underestimates of CopI/CopT complex stability, if appreciable dissociation takes place during electrophoresis. We therefore attempted to obtain an independent estimate of K_d values. Rate constants of formation (k_1) and dissociation (k_{-1}) of CopI/CopT pairs, as well as the equilibrium dissociation constant ($k_{-1}/k_1 = K_d$) can be obtained kinetically as shown by Persson *et al.* (27; Material and Methods). In principle, a K_d value can be approximated accurately in solution, if one measures the inhibitory effect of CopI on the binding of CopA to CopT. CopI/CopT kissing complex formation is permitted to reach an equilibrium in a preincubation step, and subsequently the fraction of remaining, free CopT is measured by determining its pairing rate to full length CopA. This approach worked for wild-type RNAs (27). However, the truncated CopA species used by Persson *et al.* (27) was able to form stable duplexes with CopT, albeit at a greatly reduced rate. The use of CopI essentially abolished this complication, and no appreciable CopI/CopT duplexes were formed even after long preincubation periods. Using concentrations of CopI that were close to the K_d values shown in Table 1, we attempted the inhibition experiment for all homologous mutant and wild-type RNAs (Materials and Methods). These experiments yielded K_d values of 1.6 × 10^{-9} M (wild-type) and 5 × 10^{-11} M (mutant 6C). These values are four to eight times lower than the ones obtained by the native gel assay (Fig. 3; Table 1), indicating that some dissociation of the kissing complex may have occurred in the gel. The value for the wild-type CopI/CopT pair is much higher than

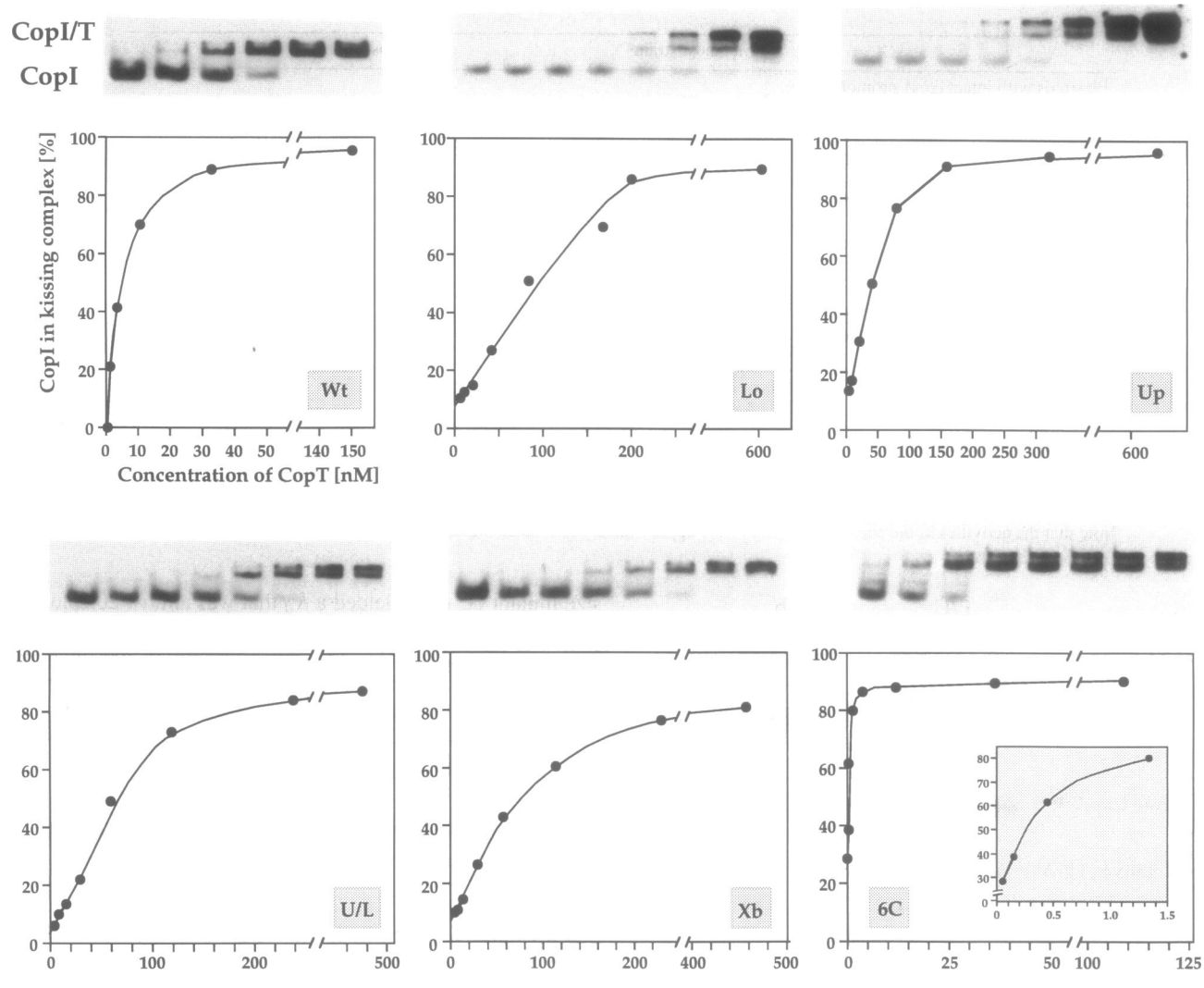

Figure 3. Determinations of relative equilibrium dissociation constants of homologous CopI/CopT pairs. Uniformly labelled CopI was incubated with different concentrations of tritiated CopT, and native gel electrophoresis was performed as described in Materials and Methods. For each homologous CopI/CopT pair, autoradiograms of dried gels are shown, and below the quantitation of kissing complex formation is graphically depicted. The insert in the '6C' graph shows a segment of the same curve with an expanded x-axis.

that calculated previously (27). We interpret the earlier values to be underestimates, most likely due to additional inhibition by the short single-stranded extensions of the truncated CopA, in particular the 3′-tail.

Unfortunately, the kinetic K_d determination was not feasible for the bulge mutant RNAs, as we failed to see substantial inhibition at the expected CopI concentrations for mutants -Lo, -Up, -L/U and -Xb. This was apparently due to CopI multimerization at high concentrations (data not shown). Thus, only wild-type and mutant 6C could be analyzed with confidence, since at the low concentrations required for inhibition, multimerization did not occur to any significant extent.

Bulge mutations abolish CopA-mediated inhibition of *repA-lacZ* expression

In order to see whether the decreased *in vitro* pairing rates of the bulge mutant CopAs correlated with impaired inhibitory activity *in vivo*, we measured *repA-lacZ* expression from plasmids carrying the wild-type or mutant *copA* genes. The plasmids of the pGW177-L-series carry translational *repA-lacZ* fusions on a p15A-plasmid vector (3). The mutant *copA* alleles were introduced as described in Materials and Methods. RepA-LacZ fusion protein synthesis was measured in extracts of cells harboring these plasmids, and represents antisense RNA-regulated expression. To analyze derepressed RepA-LacZ synthesis, the *copA* promoter-down mutation III (23,24) was introduced into the wild-type plasmid, pGW177-L, and one mutant plasmid, pGW177-L/U-L, to yield pGW177-III-L and pGW177-III-L/U-L, respectively.

Since some of the bulge mutations resulted in an RNAse III-dependent decrease in steady-state CopA level [see accompanying paper (20)], we also tested *repA-lacZ* expression in an *rnc* mutant strain. The results are shown in Table 2. All mutations increased *repA-lacZ* expression compared to that obtained with the wild-type fusion plasmid. This is true in both strain

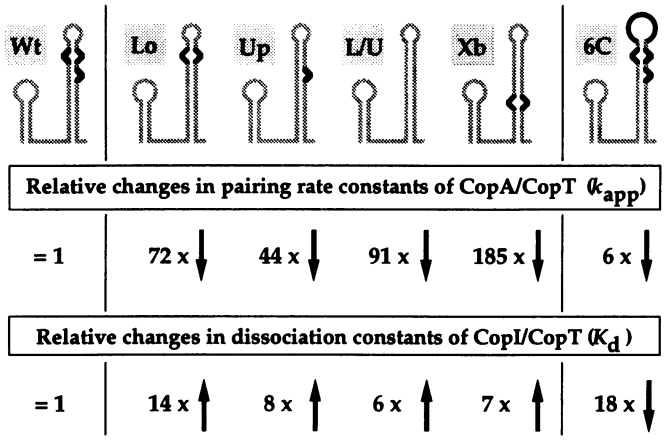

Figure 4. Schematic representation of CopA/CopT pairing rates and relative CopI/CopT equilibrium dissociation constants. CopA RNAs are depicted as shaded lines, and the relevant structural features in the mutant and wild-type cases are highlighted by solid lines. Changes in pairing rate constants or dissociation constants were taken from Table 1. The direction of the change is indicated by arrows.

backgrounds, even though β-galactosidase activities were generally higher in the *rnc*-strain, as demonstrated previously (30). In particular, in the absence of RNase III, *repA-lacZ* expression is derepressed in the absence of CopA in an otherwise wild-type fusion plasmid (cf. pGW177-L and pGW177-III-L, Table 2), whereas derepressed RepA synthesis occurs from the bulge mutant L/U-plasmid whether or not CopA is present (cf. pGW177-L/U-L and pGW177-III-L/U-L, Table 2). Very low inhibiton was also seen when a larger excess of the mutant CopAs was provided from a second plasmid *in trans* (data not shown). Thus, we infer that all bulge mutations cause an impairment of CopA's inhibitory capacity, in accord with the strong effects upon pairing rates demonstrated above (Fig. 1; Table 1).

DISCUSSION

In this paper we address the functional significance of bulged-out nucleotides for antisense RNA-mediated inhibition. We used the CopA/CopT system of plasmid R1 as a model and performed *in vitro* and *in vivo* experiments to assess the effect of bulges/internal loops on the effectiveness of antisense RNA control. CopA mutant RNAs were generated in which upper stem helicity was restored at the position of the upper bulge (Up), the lower bulge (Lo), or both (L/U). An additional CopA variant was engineered to contain the L/U mutation and in addition two consecutive base changes resulting in a new internal loop at greater distance from loop II (CopA-Xb). The presence or absence of the expected structural alterations were verified by enzymatic and chemical probing (20).

Pairing rate determinations with homologous CopA/CopT pairs showed that all mutations caused drastic reductions in the pairing rate constant, k_{app}, ranging from ~44–185-fold lower values than that of the wild-type (Fig. 1; Table 1). Since previous analyses have shown that binding occurs in at least two distinguishable steps, we also tested the stability of kissing intermediates. Kissing complexes between CopI (a truncated CopA that can only proceed to an extended loop–loop binding intermediate; 26) and CopT were analyzed on native gels to obtain relative K_d values. Mutation-dependent defects were similar to those obtained in the pairing assay (6- to 14-fold; Fig. 3; Table 1), but K_d values were quantitatively much less affected than k_{app} values (Fig. 4). Bulge mutants Lo and L/U were found to be most severely affected in both pairing and kissing complex stability. Attempts to determine K_d values indirectly, by measuring kissing complexes kinetically in a pairing inhibition assay, proved not feasible (see Results). For a wild-type CopI/CopT pair, the two methods yielded equilibrium dissociation constants of $\sim 7 \times 10^{-9}$ M (native gel assay; Fig. 3; Table 1) and 1.6×10^{-9} M (pairing inhibition, see Results), respectively. Since the values measured for the mutant 6C pair show approximately the same method-dependent difference, we assume that dissociation during gel electrophoresis may be responsible for the higher calculated K_d values.

Inhibition of *repA-lacZ* by CopA was assayed in strains proficient or deficient in RNase III. In the accompanying paper, we showed that, in particular, CopA-Lo and CopA-L/U were degraded in an RNase III-dependent manner. Therefore, fusion protein synthesis in a wild-type host strain measures CopA-dependent inhibition of RepA-LacZ synthesis both dependent on antisense RNA stability and of the binding rate constants, whereas in the *rnc* mutant strain the contribution of binding rate constants to inhibition is primarily assessed. All bulge mutant CopAs are poor inhibitors (Table 2), in accord with respective pairing rates *in vitro* (Fig. 1; Table 1). Since a restoration of metabolic stability of CopA-Lo and CopA-L/U [see accompanying paper (20)] in the *rnc*$^-$ strain still resulted in derepressed RepA-LacZ synthesis, we conclude that loss of CopA activity in the bulge mutant constructs is predominantly due to the severe decrease in their binding rate constants.

Antisense RNA mutants have been investigated in other systems, and the effects of several mutations are relevant to the present analysis. The replication inhibitor of plasmid pMU701, RNAI, has recently been analyzed with respect to binding process and inhibition (13,16). RNAI consists of one stem–loop, with a six-base loop sequence identical to that of CopA. The upper stem appears to be base-paired, but two non-canonical U:U base pairs and a G/A internal loop suggest that this region is destabilized (16). Four mutations in RNAI [denoted: U43G, U34G, U33G and A47U; (16)] were predicted to stabilize the upper stem. All of these resulted in increased plasmid copy numbers. Siemering *et al.* (13) propose that the inhibitory effect of RNAI is dependent on an extended kissing complex, similar to the one proposed for CopA/CopT (26), and that its formation is facilitated by a destabilizing element in the upper stem. In contrast to CopA/CopT, RNAI and RNAII appear to form complete RNA duplexes very slowly, so that both the rate of formation of the intermediate and its stability should effect inhibition. In both IncB and IncIα-plasmids, once this intermediate forms, inhibition of Rep synthesis is established, since this structure sequesters target sequences needed to form an activator pseudoknot that is required for Rep protein translation (5–7).

Kittle *et al.* (17) studied pairing between RNA-OUT and RNA-IN of *IS*10. RNA-OUT consists of one single stem–loop without single-stranded tails of significant length, and carries several unpaired bases within the upper stem region. Binding occurs in a 'one-step mode', i.e. once the single-stranded 5′-end of RNA-IN has initiated binding to RNA-OUT loop bases, the short helix is propagated by strand migration towards the RNA-OUT 5′-end. A mutation predicted to close an internal loop,

extending the top-most 3 bp into 6 consecutive bp (*mci1*; 17), practically inactivates RNA-OUT with respect to pairing *in vitro* and inhibition *in vivo*. This is due to a change in structure rather than sequence, since *mci1* RNA-OUT is inactive on both mutant and wild-type targets, whereas wild-type RNA-OUT is active on both homologous and heterologous targets (17).

RNAI of ColE1 also carries irregular helical segments within two of its stem–loops. However, it is unclear whether kissing or pairing is dependent on these bulges. Eguchi and Tomizawa (31) showed that a kissing complex between single stem–loops III (carrying a bulged nucleotide 3 bp from the loop) of both the antisense and target RNA is 40–50 times more stable than the corresponding pairs of stem–loops I and II. Whether this difference reflects the effect of bulge-dependent destabilization of the former two reactant RNAs is unclear, since Eguchi and Tomizawa (32) have demonstrated that changes in loop sequences can have drastic effects on dissociation rates of stem–loop pairs.

From the results described here and those discussed above, we conclude that binding intermediates formed between complementary stem–loops are more stable if helix-destabilizing elements are present in upper stem regions. This is not surprizing, since the introduction of bulges and internal loops will favor inter-strand helix formation over imperfect intra-strand base-pairing. Thus, removal of bulges may impair inter-strand helix propagation into the upper stem and result in higher dissociation constants of the kissing RNA pair. Whether the stability of loop–loop binding intermediates is directly correlated with antisense/target RNA pairing rates and/or inhibition rates will depend on the properties of the system studied. In ColE1 and R1, the rate-limiting step for RNA pairing is the formation of an early kissing intermediate (for reviews, see 10,33). Mutations in loops of RNAI/ColE1 and CopA/R1 generally cause small changes in the pairing rate constant of the mutant compared to the wild-type pair, although the predicted K_d change of mutant versus wild-type can be large (e.g. 10,12). A pathway in which binding is essentially diffusion-controlled follows Briggs–Haldane kinetics; i.e. early binding intermediates (kissing complex) will not dissociate within the time span required to commit the molecules to product formation (initiation of stable pairing). Therefore, large changes in loop–loop K_d values are expected to contribute relatively little to overall pairing rates, since the dissociation rate constant k_{-1} of the intermediate is very small compared to the hybridization rate constant k_2 (10).

Thus, the effects of bulge mutations on pairing and kissing are difficult to interpret. The qualitative correlation between bulge mutation-dependent increase in K_d and decrease in k_{app} could suggest that the transiently formed CopA/CopT intermediate (i.e., the kissing complex) has to be sufficiently stable for pairing to proceed. However, the quantitative difference between k_{app}- and K_d-effects indicates that, as expected, binding affinity does not directly determine pairing rate. This is emphasized by mutation 6C. An 8 nt CopA loop with six consecutive C-residues resulted in a kissing complex of higher than wild-type stability, even though k_{app} was decreased (Table 1; Fig. 4). Thus, we cannot unambiguously identify the cause of the pairing defects in the bulge mutants. However, decreases in k_{app} of all bulge mutations were strikingly large compared to the small k_{app} changes associated with loop sequence mutations (12,25; Wagner, unpublished). We propose that the adverse effects on pairing rates may be due to secondary and tertiary structure changes in regions crucial for proper presentation of recognition loops. Alternatively, after kissing has occured, a putative structural rearrangement required for initiation of stable pairing may be prevented. In this respect, it is suggestive that the two most affected mutant CopAs (Lo and L/U) showed greatly altered gel mobility [see accompanying paper (20)]. Additionally, we have to consider that bulge mutant CopAs may follow an altogether different binding pathway, in which initiation of binding may not primarily occur at the loops. The very low pairing rate constants in the 10^4 M^{-1} s^{-1} range are compatible with this, since some artificial antisense/target RNA pairs yielded similar k_{app} values. Recently, Thisted *et al.* (34) have shown that Sok/SokT binding initiates in the single-stranded tail region instead of at the loops, resulting in k_{app} values around 10^5 M^{-1} s^{-1}. Thus, bulge mutant CopAs may initiate pairing in the single-stranded region inbetween the CopA stem–loops, and loop–loop binding may be non-productive.

Irrespective of the details of the binding pathway, we propose that the removal of the bulges essentially inactivates CopA. However, the presence of bulges or internal loops *per se* is not sufficient for activity, since CopA-Xb was ineffective as well. This indicates that antisense RNAs like CopA (and others, see above) appear to have evolved structures for optimal performance. Binding rate is a major determinant for inhibitory efficiency. We conclude that, in addition to primary loop sequence (12), loop size or structure (25), and the presence of single-stranded regions for initiation of stable pairing (26), bulges and internal loops at specific positions within stem–loop II are required for maximum binding rates and inhibition. This suggests that optimal artificial antisense RNA design should attempt to incorporate such elements.

ACKNOWLEDGEMENTS

We thank L. Kirsebom for synthesis of oligodeoxyribonucleotides. We are grateful to K. Nordström and D. Andersson for critical reading of the manuscript. This work was supported by The Swedish Natural Science Research Council and the Swedish Board for Technical Development.

REFERENCES

1 Wagner, E.G.H. and Simons, R. (1994) *Annu Rev. Microbiol.* **48**, 713–742.
2 Tomizawa, J. and Itoh, T. (1981) *Proc. Natl. Acad. Sci. USA* **78**, 6096–6100.
3 Blomberg, P., Nordström, K. and Wagner, E.G.H. (1992) *EMBO J.* **11**, 2675–2683.
4 Wu, R., Wang, X., Womble, D.D. and Rownd, R.H. (1992) *J. Bacteriol.* **174**, 7620–7628.
5 Asano, K., Kato, A., Moriwaki, H., Hama, C., Shiba, K.A. and Mizobuchi, K. (1991) *J. Biol. Chem.* **266**, 3774–3781.
6 Asano, K., Moriwaki, H. and Mizobuchi, K. (1991) *J. Biol. Chem.* **266**, 24549–24556.
7 Wilson, I.W., Praszkier, J. and Pittard, A.J. (1993) *J. Bacteriol.* **175**, 6476–6483.
8 Novick RP, Iordanescu S, Projan SJ, Kornblum J, Edelman I. (1989) *Cell* **59**, 395–404.
9 Brantl, S., Birch-Hirschfeld, E. and Behnke, D. (1993) *J. Bacteriol.* **175**, 4052–4061.
10 Nordström, K. and Wagner, E.G.H. (1994) *Trends Biochem. Sci.* **19**, 294–300.
11 Tomizawa, J. (1984) *Cell* **38**, 861–870.
12 Persson, C., Wagner, E. G. H. and Nordström, K. (1988) *EMBO J.* **7**, 3279–3288.
13 Siemering, K.R., Praszkier, J. and Pittard, J.A. (1994) *J. Bacteriol.* **176**, 2677–2688.

14 Sugiyama, T. and Itoh, T. (1993) *Nucleic Acids Res.* **21**, 5972–5977.
15 Wagner, E. G. H. and Nordström, K. (1986) *Nucleic Acids Res.* **14**, 2523–2538.
16 Siemering, K.R., Praszkier, J. and Pittard, J.A. (1993) *J. Bacteriol.* **175**, 2895–2906.
17 Kittle, J.D., Simons, R.W., Lee, J. and Kleckner, N. (1989) *J. Mol. Biol.* **210**, 561–572.
18 Twigg, A. and Sherratt, D. (1980) *Nature* **283**, 216–218.
19 Tomizawa, J. and Som, T. (1984) *Cell* **38**, 871–878.
20 Hjalt, T.H. and Wagner, E.G.H. (1994) *Nucleic Acids Res.* **23**, 571–579.
21 Casadaban, M.J. and Cohen, S. N. (1980) *J. Mol. Biol.* **138**, 179–207.
22 Plumbridge, J. A., Dondon, J. and Nakamura, Y. (1985) *Nucleic Acids Res.* **13**, 3371–3388.
23 Öhman, M. and Wagner, E.G.H. (1991) *Mol. Gen. Genet.* **230**, 321–328.
24 Blomberg, P., Engdahl, H.M., Malmgren, C, Romby, P. and Wagner, E.G.H. (1994) *Mol. Microbiol.* **12**, 49–60.
25 Hjalt, T. and Wagner, E. G. H. (1992) *Nucleic Acids Res.* **20**, 6723–6732.
26 Persson, C., Wagner, E. G. H. and Nordström, K. (1990) *EMBO J.* **9**, 3767–3775.
27 Persson, C., Wagner, E. G. H. and Nordström, K. (1990) *EMBO J.* **9**, 3777–3785.
28 Pyle, A.M., McSwiggen, J.A. and Cech, T.R. (1990) *Proc. Natl. Acad. Sci. USA* **87**, 8187–8191.
29 Berzal-Herranz, A., Wagner, E.G.H. and Díaz-Orejas, R. (1991) *Mol. Microbiol.* **5**, 97–108.
30 Blomberg, P., Wagner, E. G. H. and Nordström, K. (1990) *EMBO J.* **9**, 2331–2340.
31 Eguchi, Y. and Tomizawa, J. (1990) *Cell* **60**, 199–209.
32 Eguchi, Y. and Tomizawa, J. (1991) *J. Mol. Biol.* **220**, 831–842.
33 Eguchi, Y., Itoh, T. and Tomizawa, J. (1991) *Annu. Rev. Biochem.* **60**, 631–652.
34 Thisted, T., Sørensen, N.S., Wagner, E.G.H. and Gerdes, K. (1994) *EMBO J.* **13**, 1960–1968.